April 2011

Construction and Analysis of a Gain-of-Function PCV2 VP3 Isoform Chimera

Andrew Francis Nemeth
Worcester Polytechnic Institute

Courtney Lynne Gilbert
Worcester Polytechnic Institute

Construction and Analysis of a Gain-of-Function PCV2 VP3 Isoform Chimera

A Major Qualifying Project

Submitted to the Faculty
of the
WORCESTER POLYTECHNIC INSTITUTE

In Partial Fulfillment of the Requirements for the
Degree of Bachelor Science

By:

Andrew Nemeth

Courtney Gilbert

Date: April 25, 2011
Approved:

Professor Destin Heilman, Primary Advisor

Abstract:

The chicken anemia virus protein Apoptin is able to selectively induce apoptosis in transformed cells while leaving primary cells intact. The mechanism of this selection is currently unknown. The product of the third open reading frame of PCV2 has a high degree of homology with the chicken anemia virus protein Apoptin, and has two naturally-occurring isoform, PCV2a and PCV2b. PCV2b displays dramatically higher apoptotic ability over PCV2a, despite the high degree of homology between the two; there is a difference of only two amino acids between PCV2b and PCV2a. To determine the role of the two different amino acids in the induction of apoptosis, a chimeric protein was generated featuring one distinct amino acid from each isoform. Using a caspase apoptosis assay, apoptotic ability of this chimeric protein was assessed. A clearer understanding of the functionality and apoptotic mechanisms of these proteins in transformed cells may lead to therapeutic applications for cancer.

Acknowledgements:

We would like to thank Dr. Destin Heilman for his unending patience and wisdom in guiding us through this research. We would also like to thank our lab mates for their camaraderie and support.

Table of Contents:

Introduction:

Porcine circovirus type 2 (PCV2) is a virus of the family *Circoviridae. Circoviridae* are a family of viruses that are characteristically small, about 17-22nm in diameter. These viruses are naked icosahedral viruses with circular, single-stranded DNA genomes that code for only one capsid protein. Members of *Circoviridae* are prevalent and fairly stable in the environment. Polymerases with repair activity in their host cells use the circovirus ssDNA as the template to build the genomes that will compose progeny virions (1). The forces of viral evolution of the family *Circoviridae* seem to lead back to naturally occurring point mutations and recombination (2).

PCV2 belongs specifically to the *Circovirus* genus of the *Circoviridae* family. It is commonly found in swine, and is the causative agent for post-weaning multisystemic wasting disorder (PWMD (1). PCV2 consists of an icosahedral protein capsid and a single-stranded circular DNA genome consisting of approximately 1.76kb (3). It is non-enveloped and 17nm in diameter, both typical features of members of the family *Circoviridae.* (4). PCV2's is composed of protein coat subunits assembled in 12 pentameric units (5). The multiple routes for the transmission of PCV2 from pig to pig include nasal, oral, and fecal cavities. The virus may be present in any excretions or secretions of an infected pig, and is easily spread through entire swine groups (6).

The PCV2 genome consists of six open reading frames, three of which are functional and are used to produce four different proteins: Rep, rep', capsid, and VP3. Both the rep and rep' proteins form PCV's replicase complex; these two proteins recognize each other and have been shown to interact with each other at the hair-pin loop at the origin of replication, thus initiating

replication (7). The capsid protein forms the protein viral coat. The VP3 protein proves to be unique from the other three proteins; it is involved in neither viral genome replication nor formation of the viral protein capsid (19). This product of PCV2's third open reading frame plays a central role in inducing cellular apoptosis in its host cells, allowing rapid of spread of progeny virions; previous research has proven VP3 necessary for viral pathogenesis (8).

Two isoforms of PCV2 exist; they are PCV2a and PCV2b. The two isoforms show significant homology to one another. Their genomic nucleotide sequences differ by only 5%. They both produce the same four proteins of their six open reading frames (9). Of the two isoforms, PCV2b is the virulent isoform associated with the high mortality rates among swine through induction of cellular apoptosis; the PCV2a isoform is considered nonpathogenic (10). The difference in killing capacity between PCV2a and PCV2b is believed to be a result of two point mutations in two putative domains, one of which is the protein's nuclear export sequence (located towards the N terminus), and the other is the protein's localization/multimerization sequence (featured towards the C terminus) which also contains the phosphorylation site. The nonpolar glycine at position 41 of the PCV2a peptide chain is replaced by a polar serine in PCV2b, in addition to the replacement of an aromatic phenylalanine at the very end of the PCV2a protein with an aliphatic leucine in PCV2b. This difference seems to confer the increased apoptotic capacity and subsequent lethality of the "b" isoform (11).

PCV2's protein product of its third open reading frame, VP3, demonstrates considerable homology to chicken anemia virus (CAV) VP3. CAV VP3, also referred to as Apoptin, has been identified as a novel protein with the capacity to induce apoptosis in transformed cells only, leaving primary cells intact. The detailed mechanism by which Apoptin selectively causes apoptosis has not yet been elucidated, but is widely thought to be due in some part to differential

localization of Apoptin: in transformed cells it tends to localize in the nuclear space, and in primary cells it localizes in the cytoplasm. The method by which this selective apoptosis takes place via Apoptin is thought to be due to the induction of its shuttling between the cytosol and nuclear space. Movement of CAV Apoptin out of the nucleus and into the cytoplasm allows its interaction with anaphase promoting complex/cyclosome (APC/C) of the host cell. Upon exiting the nucleus, Apoptin is able to interact with APC1 leading to inhibition of APC/C. This in turn leads to the host cell entering cell cycle block leaving itself trapped in the G_2M stage resulting in apoptosis (12). This pathway results in p53-independent cell death. In addition to this, it has been speculated that apoptotic induction by Apoptin is part of a mitochondrial death pathway. Apoptin has been shown to be associated with cytochrome C release from mitochondria which causes subsequent caspase 3 and 7 activation and formation of apoptosome. In the process of apoptosome formation, cytochrome C interacts with the protein Apf-1 to disable the auto-inhibition of Apf-1's WD-40 domain, allowing further quaternary structure formation wherein ATP can bind to the structure to disinhibit the CARD domain. Once the CARD domain has been exposed, the structure can then complex with caspase 9, whose activity induces the total caspase cascade, ultimately inducing apoptosis (13).

Still, however, the killing ability of Apoptin does not seem to be due solely to nuclear localization; the protein is also suspected to have the ability to multimerize, which may play a role in its apoptotic ability (13). The primary evidence for this multimerization capability lies in the punctate appearance of Apoptin in fluorescence localization studies in which it is conjugated with green fluorescent protein. The structural motif responsible for Apoptin's tendency to aggregate into multimers has been mapped to the hydrophobic interactions of the N-terminal half of the protein. Apoptin's globular aggregation is strong and practically irreversible. In addition to

this, research conducted by Leliveld et.al suggests that Apoptin's killing capacity does not lie within specific secondary structures among the multimer; rather, semi-random aggregation seems to be adequate to induce apoptotic activity among host cells (14).

CAV Apoptin and PCV2 VP3 show considerable degrees of homology. This homology between the better-studied Apoptin of avian anemia and PCV2 VP3 is significant, making present research regarding of Apoptin useful for a stronger understanding of PCV2 VP3. Prior research has indicated that PCV2 VP3 may also selectively induce apoptosis in a similar fashion, suspected due to its homology with CAV Apoptin. It is similar to Apoptin in that it is believed to be able to mulitmerize with itself, in addition to having a sequence for nuclear export (15).

VP3 functions in triggering cell death via a p53-dependent pathway. PCV2 VP3 has been demonstrated to interact with the porcine ubiquitin protein pPirh2. The ubiquitin pPirh2 has the ability to complex p53 and induce its degradation through proteosomic signaling. This yields a possible mechanism for PCV2's killing capacity; by causing an increase in p53 levels through inhibition of its ubiquitylation, the apoptotic process is induced. Through yeast-two-hybrid experiments as well as localization and co-immunopreciptation studies, a definite physical interaction PCV2 VP3 and the p53-binding-domain of Pirh2 was demonstrated. (16). The activation of an apoptosis-inducing gene is regulated by phosphorylation of the p53 serine residue at position 146. This possible mechanism has been corroborated by studies in which PCV-infected and ORF3-transfected cells show increased expression, thus leading to higher likelihood of p53 phophorylation and therefore up-regulation of apoptosis (17).

Additionally, infection with PCV2 appears to differ from Apoptin with regard to its activation of the JNK1/2 and p38/MAPK (Mitogen-Activated Protein Kinsae) pathways, which

serve to regulate the host cell apoptotic pathway for a wide variety of viruses. Research conducted by Liu, et.al led to speculation that phosphorylation of JNK causes p53 to dissociate from it. PCV2's ability to modulate these two cell-signaling pathways depends on PCV2's replication; UV-irradiated PCV2 along with PCV2 in its early infection stages proved unable to interact with the aforementioned pathways. Under ample enough replication of the virus, however, this activation further enhances expression of p53 and also stabilizes its activity by preventing its proteosomal degradation. Enhancing the pPirh2-mediated up-regulation of p53 by inhibition of ubiquitylation even further leads drives the host cell to an apoptotic pathway (17).

In spite of this mechanistic research, previous in-house research has shown that PCV2b VP3 also demonstrates functionality in p53-null cell lines, implying that there may be another pathway by which PCV2b VP3 induces apoptosis.

The negative effects of PCV2 provide great incentive for further research on the pathogenicity of this virus. Investigation into the mechanistic details of VP3's apoptotic selection is of central interest to this study. The practical focus of the current research was to introduce a gain-of-function mutation into PCV2a via two mutually exclusive cloning strategies, site-directed mutagenesis and ligation cloning. Exploration of the chimera's killing ability would perhaps reveal characteristics of PCV2 responsible for inducing apoptosis in transfected cells.

Materials and Methods:

Overlap Extension Polymerase Chain Reaction

Pyrococcus furiosus polymerase was used in conjunction with mutagenic primers containing the complement of PCV2B's NES amino sequence difference to generate the chimeric protein product. DNA stocks of PCV2A were placed in serial dilutions from 50 ng/μL to 6.25 ng/μL. 2 μL of resuspended forward and reverse primers was added to DNA in 1 μL Pfu buffer with purified Millipore water added to make a total volume of 50 μL. 18 cycles of PCR were run at the following temperatures: cycle 1 at 95°C for 30 seconds, cycle 2 at 95°C for 30 seconds, cycle 3 at 55°C for 1 minute, cycle 4 at 68°C for 10 minutes (2 minutes * 5 kilobase for total plasmid length), repeat cycles 2-4 five times, rest at hold temperature of 4°C for a total of 17 cycles.

Confirmation of PCR Product

This product was then digested with dpn1 via addition of 1 μL dpn1 to each PCR product tube and incubation at 37°C for an hour. The restriction was then run on an agarose gel, prepared by dissolving .45 g of agarose in 50mL of sterile 1x TAE and microwaving for one minute, then pouring into gel tank. When the gel solidified, the gel tank was filled with sterile 1x TAE to a level slightly below the top of the solidified gel. The wells were filled with restriction mixture and the voltage set to 90V.

PCR product DNA was then scaled up by mid-sized culture. 3 μL of PCR product was pipetted into thawed supercompetent JM109 *E.coli.* DNA-membrane complexes were allowed to form for 25 minutes while the tubes were on ice. Cultures then transferred into a 42°C bath for exactly 60 seconds for a heat-kill to make *E.coli* membrane more permeable. The eppendorf tubes were then transferred into ice for 2 minutes to help the membranes re-form. To aid in

recovery, 450 μL of LB media was added to each culture tube and allowed to rotate in an incubator-shaker at 37°C for an hour. A mixture of recovery media with the antibiotic kanamycin was prepared by adding 500 μL of 1000x kanamycin into 500 mL of autoclaved LB media. The recovered cultures were pipetted into 150 μL LB with kanamycin in autoclaved 500mL erlenmeyer flasks and allowed to proliferate overnight in the incubator-shaker at 37°C and 220 revolutions per minute.

Midiprep of cultures was performed using Promega Wizard Midiprep Kit. 100 mL of cells in each tube were pelleted at 10,000 x g for 10 minutes at 4°C. The supernatants were removed and the pellets were re-suspended in 3 mL of Cell Resuspension Solution. 3 mL of Cell Lysis Solution was added to each tube and inverted to mix. Next, 3 mL of Neutralization Solution was added and tubes were again inverted to mix. The tubes were centrifuged at 14,000 x g for 15 min. at 4°C and the supernatant containing DNA was recovered and transferred to new tubes. Purification Resin (10 mL) was added to each tube and mixed by swirling. Using the Midicolumn and vacuum, the DNA/Resin mixture was pushed through the column. 15 mL of Column Wash Solution with ethanol was also pushed through the column two separate times and the pellet was allowed to vacuum dry for 30 sec. after all the liquid had left the column. The column was then removed, placed in an eppendorf tube, and then centrifuged for 2 min. at 10,000 x g. The column was placed in a new eppendorf tube and 300 μL of prewarmed (~70° C) ddH_2O was added and allowed to sit for 1 min. After, the tubes were centrifuged for 20 sec. at 10,000 x g to elute the DNA. The Midicolumns were then discarded and the eppendorf tubes were centrifuged again, this time at 10,000 x g for 5 min. to pellet the resin. The supernatants were collected and transferred to new tubes, resuspended in 50 μL of TE and stored at -20° C.

A standard restriction profile was performed by adding 1 μL Buffer C, 1 μL Buffer H, 1

μL PCV2a or PCV2b DNA, 1 μL SacII restriction enzyme, and 1 μL EcoRI restriction enzyme in the order presented. Two controls lacking one restriction enzyme each were created using PCV2a DNA to ensure thorough restriction profiling. These restrictions were allowed to incubate in a 37°C water bath for an hour. A gel of these restrictions was run in the manner described previously.

Transfection of H1299 Cell Line

A 96-well plate was colonized with H1299 cells. H1299 non-small lung cell carcinoma cells were transfected using the Qiagen Effectene Transfection protocol using a variety of PCV2 VP3 constructs. The first and second wells were transfected with the wild type A and B PCV2 VP3 isoforms. Subsequently, the third and fourth sets of wells were transfected with the NES and NLS truncation mutant constructs of the PCV2A isoform.The final column of wells was transfected with our chimeric PCV2A-B VP3 protein. Each transfection was performed in quintuplicate. The transfected H1299 cells were incubated in the standard conditions growth conditions of 37°C and 5% CO_2 in Dulbecco's Modified Eagle's Medium (DMEM) with 10% fetal bovine serum (FBS) and PSF as an antibiotic (containing penicillin, streptomycin, and fungizone). Construct DNAs were combined with 150 μL Buffer EC. 4 μL of Enhancer was added to each and the mixtures were mixed by hand. These were incubated at room temperature for 5-10 minutes. Approximately 170 μL of the media was removed from each well, and 30 μL of the transfection complexes were added dropwise. These transfections were then incubated under the standard cellular proliferation conditions for 48 hours.

Apoptosis Assay

The Apo-ONE® Homogenous Caspase-3/7 Assay from Promega was used to detect caspase enzyme activity. The caspase assay reagents were added in to transfected cells in triplicate. 50 μL of Apo-ONE Caspase-3/7 Reagent was added to each well. After 36 hours of incubation, the fluorescence emitted from each well was measured using a fluorescence spectrometer with an excitation wavelength of 488 nm and a maximum emission wavelength of 520nm.

Results

Chimeric Protein Generated

The circovirus protein PCV2B VP3's ability to induce apoptosis in transformed cells is of particular interest as a result of PCV2A VP3's high degree of homology and lack of apoptotic function (Figure 1). The discrepancies between PCV2a and PCV2b that are of interest are located in the putative NES and NLS (Figure 3). This functionally results in a difference of a glycine to serine at position 41 and a phenylalanine to leucine at position 96. In an attempt to isolate the amino acid difference which may confer killing ability, two mutually exclusive methods were used to attempt to generate a chimera of the two PCV2 VP3 proteins with the NES of one protein and the NLS of the other.

Restriction digestion and ligation was selected as a method due to its conceptual simplicity (Figure 3). This process will be used to isolate fragments of each isoform of the NLS from the GFP vector and remainder of the gene (Figure 3) so that the NLS fragments can be re-annealed to the opposite vector. The gene will be cleaved approximately 180 bases from the start of the gene by SacII and the terminus by EcoRI.

Restriction digestion of both GFP PCV2 VP3 constructs yielded a vector approximately 4.7 kilobases in length and an insert of approximately 130 base pairs (Figure 4), indicating a successful digest at the SacII and EcoRI restriction sites. Restriction digestion and ligation protocol to generate the mutants is ongoing.

Site-directed mutagenesis via overlap-extension PCR was selected as an additional method to generate the mutant due to its efficiency, ease of confirmation of success, and the low level of DNA manipulation required, lessening chances of contamination and subsequent

degradation of the DNA with nucleases. For the PCR polymerase, *Pyrococcus furiosus* was selected for its processivity, efficiency, and 3'-to-5' exonuclease proofreading activity.

Utilizing this technique, mutagenic primers containing the complement of the mutation to be imposed were synthesized (Figure 5) and annealed to plasmids which have been melted apart by heat. The temperature was briefly lowered for Pfu polymerase to extend both primers completely around the plasmid (Figure 9), creating a full complement to the melted strand which includes the mutation. The process of melting apart and extending fragments of the plasmid was repeated for 18 cycles to generate many copies of the mutated plasmid. Following PCR, the product of the reaction was treated with dpn1 (Figure 6), a restriction endonuclease which recognizes and degrades a short sequence within the plasmid only if it has been methylated. Methylation of DNA occurs in *E.coli* as a way to reduce exogenous plasmid expression and also to differentiate between template and daughter DNA. As a result of the template DNA having been generated by a dam+ supercompetent *E.coli*, only template DNA was degraded, leaving the chimeric mutant DNA as the only intact plasmid in the product.

After PCR product DNA was digested with dpn1, restriction profiling in the same fashion as the restriction and ligation protocol was performed on a subsequent gel (Figure 7). This gel yielded an approximately 4-5 kilobase vector fragment and a .1-.2 kilobase insert fragment, which matches the predicted size of the restricted fragments. After DNA was scaled up via mid-sized culture and midiprep, a 1:100th dilution of the DNA was analyzed in the UV-VIS DNA spec at wavelengths of 240 and 260 nm to determine its concentration so that it could be sent out for third-party sequencing to confirm the mutation of the DNA. DNA concentration in each sample was revealed to be .807 ng/μL, .916 ng/μL, and .206 ng/μL. As .2ng/μL dilution was needed, 20 μL of the lowest-concentration midiprep was removed for sequencing as it was

already in the appropriate concentration range.

Third-party DNA sequencing (Figure 1) revealed that a guanine was substituted for an adenine at position 121, indicating that sequence of the NES of the B isoform VP3 had successfully been imposed onto the PCV2A VP3 DNA.

After the generation of the chimeric protein was confirmed, the construct was transfected into the H1299 cell line to determine both apoptotic capacity via a caspase assay and the localization of the protein. The H1299 non-small lung cancer cell line was selected as a cell line for transfection due to its prior use in conjunction with CAV Apoptin homologs and its ease of maintenance. Localization studies may confer some kind of mechanistic information regarding the protein in conjunction with apoptosis data.

Transfection after plating at 40% confluence was confirmed by expression of GFP by epifluorescence microscopy; all successful transfectants were visibly green under microscope. The wild type transfections occurred at such low efficiency that they were rendered as non-DNA transfection controls, possibly due to low initial concentration from the stock DNA. These controls underwent the same chemical treatment as the other transfectants. Apoptosis of cells was established visually (Figure 2, E and F) in cells infected with the chimeric protein. Cell membrane integrity was visibly lowered, with sections beginning to compartmentalize and bud off of the main membrane. The localization appeared to be predominantly cytoplasmic, with the nuclear region expressing less GFP and chimeric protein. Some multimerization capability was also observed as the occasional bright points of concentration of GFP. Previous studies have speculated that multimerization capability in CAV Apoptin homologs may be associated with apoptotic ability. Quantification of the fraction of apoptotic cells was unreliable due to the

rounded physiology of the other cells which may have also been in the process of apoptosis or necrosis; differentiating between non-apoptotic cells and apoptotic cells would be disingenuous.

A caspase-based apoptosis assay was performed in order to quantify apoptosis. During the process of apoptosis, effector caspases initiate a series of metabolic changes in the cell that lead to apoptosis. The apoptosis assay takes advantage of this by substituting endogenous caspase substrate with a caspase substrate which is conjugated to a fluorophore. Upon cleavage of the fluorophore with a caspase, the compound fluoresces strongly, which can be detected by fluorometry. Subsequent flurometry after incubation of the caspase assay reagents indicated that the chimeric protein, the ANES, and ANLS all had some measure of apoptotic capability (Figure 9) as indicated by the high absorbance values at 520 nm compared to the transfection controls. Background fluorescence from GFP was negligible.

Discussion:

In this study we showed that a chimeric protein construct featuring the putative nuclear export sequence of PCV2b and the functional localization sequence of PCV2a possesses apoptotic killing ability in transformed cells of the H1299 lung cancer cell line. In addition to this, we observed through microscopic imaging that the localization of the chimera is consistent with that of both wild-type forms.

Transfection of H1299 cells with the GFP-fusion chimeric constructs and subsequent apoptosis assays measured using fluorometry confirmed killing ability, as seen in Figure 8. This may suggest that PCV2b isoform's putative nuclear export sequence is largely responsible for induction of apoptosis in transformed cells. PCV2a was able to induce apoptosis with only the nuclear export sequence from the virulent isoform, and not the functional nuclear localization sequence.

Future analysis that includes quantitative data regarding the extent of apoptosis induction in the chimera versus wild-type PCV2b VP3 may help to further pinpoint the components of PCV2b VP3 responsible for its killing ability. Although the chimeric protein did show the ability to induce apoptosis in transformed cells, the degree of killing ability in the chimera versus the wild-type PCV2b VP3 has not yet been explored. If wild-type PCV2b were to display greater killing ability than the chimera, that may lead to speculation that the extent to which PCV2b is virulent depends in part on its nuclear export sequence and in part on its localization sequence. The same idea could apply to investigation of a chimeric protein construct featuring PCV2b's localization sequence with PCV2a's export sequence.

As previous research shows, PCV2a does not display killing ability in transformed cells. In addition to the above speculation regarding the nuclear export sequence of the b isoform, it may also be speculated under the current research that PCV2a shows no killing ability due to self-inhibition. Interestingly, our research may suggest that it is PCV2a VP3's structure that accounts for its inability to induce apoptosis in transformed cells. Replacing the aromatic phenylalanine in PCV2a's nuclear export sequence with the aliphatic leucine of PCV2b VP3 may be responsible for altering possible structural inhibition of wild-type PCV2a VP3. Further research that aims to structurally alter wild-type PCV2b VP3 may provide more insight on this possibility.

Our experimental transfections expressing truncations of PCV2a in H1299 cells further suggest that PCV2a inhibits itself from apoptotic ability structurally. One truncation included PCV2a's nuclear localization sequence while the other truncation featured PCV2a's nuclear export sequence. Figure 8 shows that fluorometric analysis of apoptotic assays measured increased caspase activity characteristic of apoptosis in the cells transfected with both truncations. This, again, leads to speculation that the apoptosis-inducing ability of both isoforms of PCV2 may lie in the protein's structure, and not necessarily its specific nuclear export ability or its specific localization within the cells.

Analysis of the chimeric localization in transfected cells coincided with wild-type localization patterns. However, as figure 8 demonstrates, visual results were somewhat inconclusive, as precise determination of the protein's localization was made ambiguous. The raised, spherical nature of the transfected cells due to beginning stages of apoptosis complicated the focusing of the image. While this characteristic rendered exact localization inconclusive, it

served as a visual confirmation prior to any apoptosis assay that the chimera was fully capable of inducing apoptosis.

Further investigation and revealing of the specific mechanism behind PCV2 VP3's apoptosis-inducing ability in transformed cells will be of great value to the medical field. With a considerable degree of homology between CAV Apoptin and PCV2 VP3, both hold potential for applications in anti-cancer therapeutic drugs. The more that is understood about the functional mechanisms of one, the more is understood about the other.

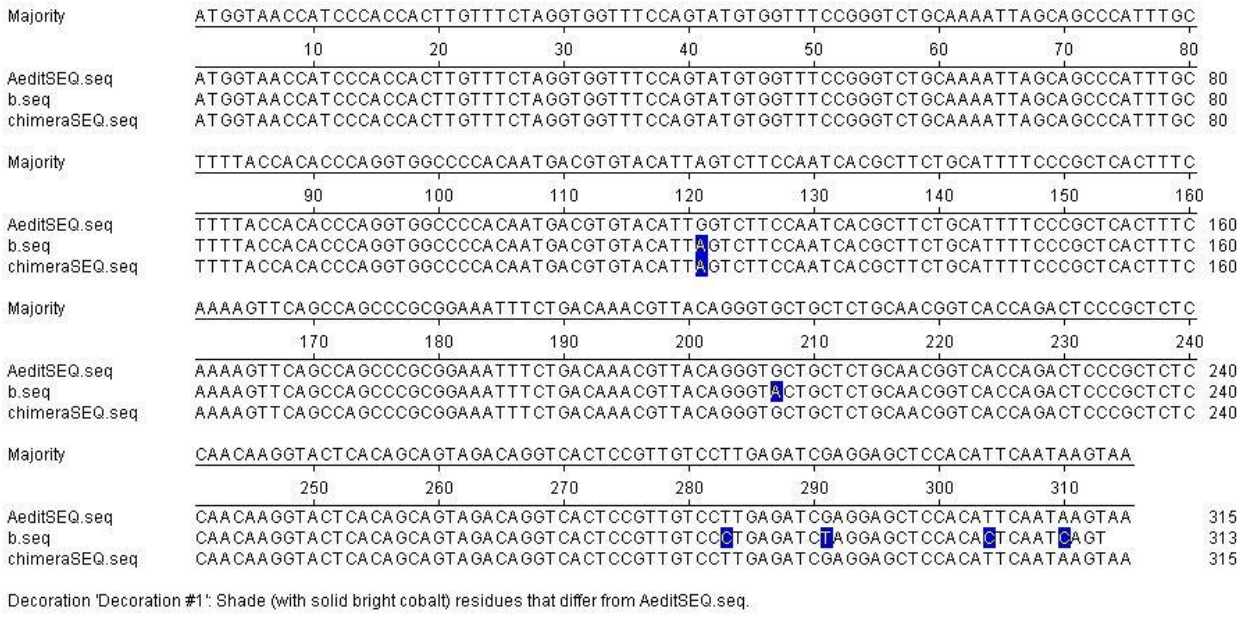

Figure 1. Site-directed mutagenesis introduces gain-of-function mutation in PCV2a VP3. Overlap-extension PCR introduces a mutation into the template PCV2a DNA which causes its NES to match that of PCV2b.

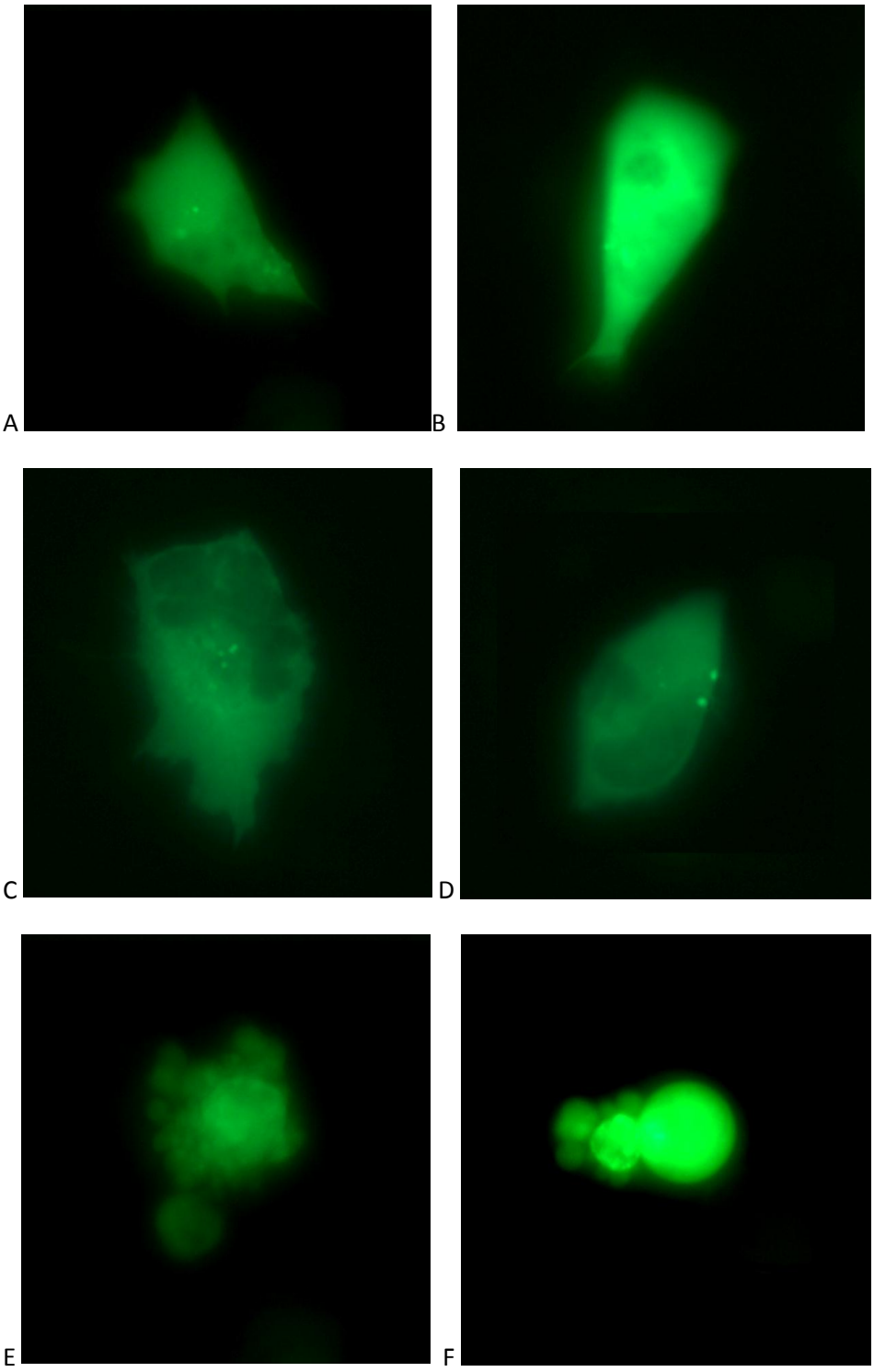

Figure 2. Epifluorescence imaging of various PCV2 VP3 mutants fused to GFP vector. Shown are NES and NLS truncation mutants (A,B), our chimeric mutant (C,D), and cells undergoing apoptosis after infection with our chimeric mutant (E,F).

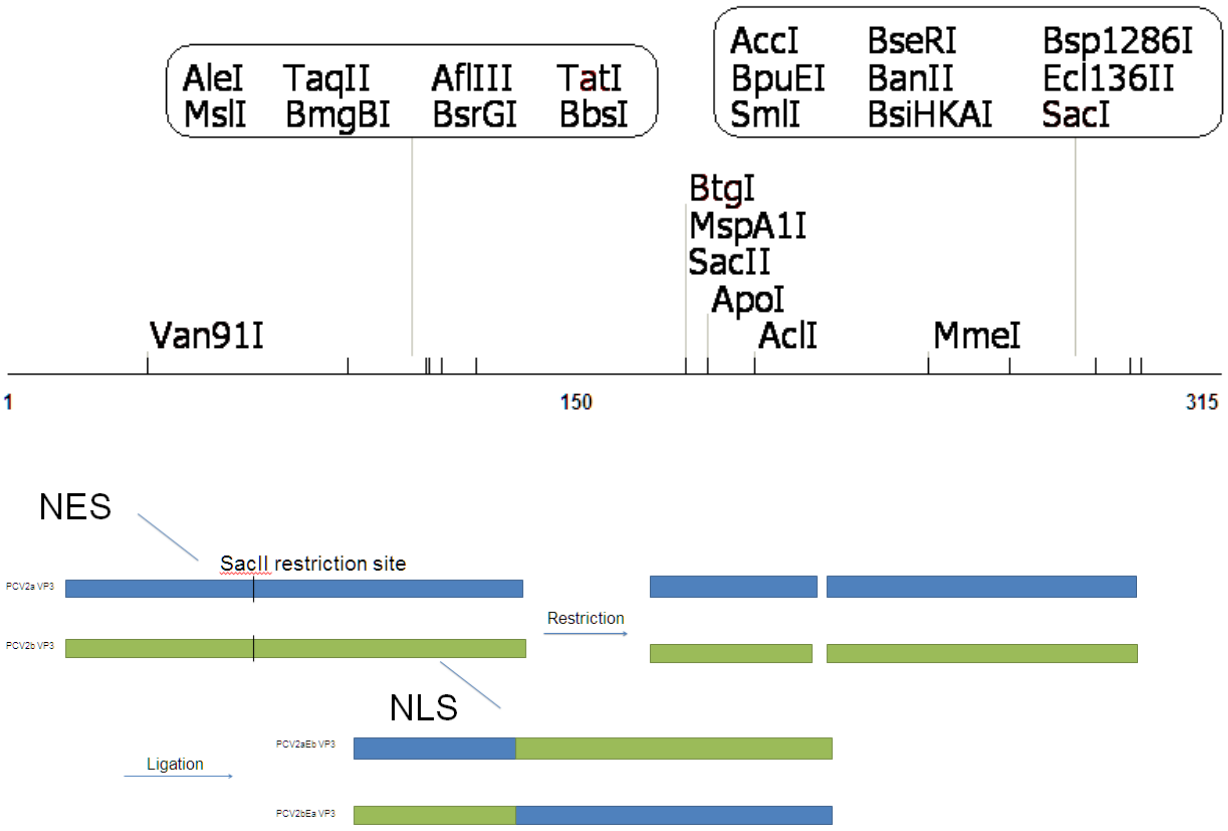

Figure 3, schematic representation of the restriction digestion and ligation protocol. The NES and NLS of the respective isoforms will be cut and swapped to generate chimeric mutants which will then be analyzed for apoptotic capability.

Figure 4, restriction profile of GFP-PCV2 constructs. Second through fourth lanes represent restricted GFP-PCV2A-VP3 DNA; fourth through seventh represent GFP-PCV2B DNA, last two lanes represent control restrictions lacking SacII or EcoRI respectively. Vector fragment (top band) resides between the 5 and 4 kilobase position markers on the ladder, while the insert fragment resides between the .1-.2 kilobase marker. The size of these fragments match the predicted 4.8 kilobase vector and 130 base insert fragment that should result from successful restriction at the SacII and EcoRI recognition sites.

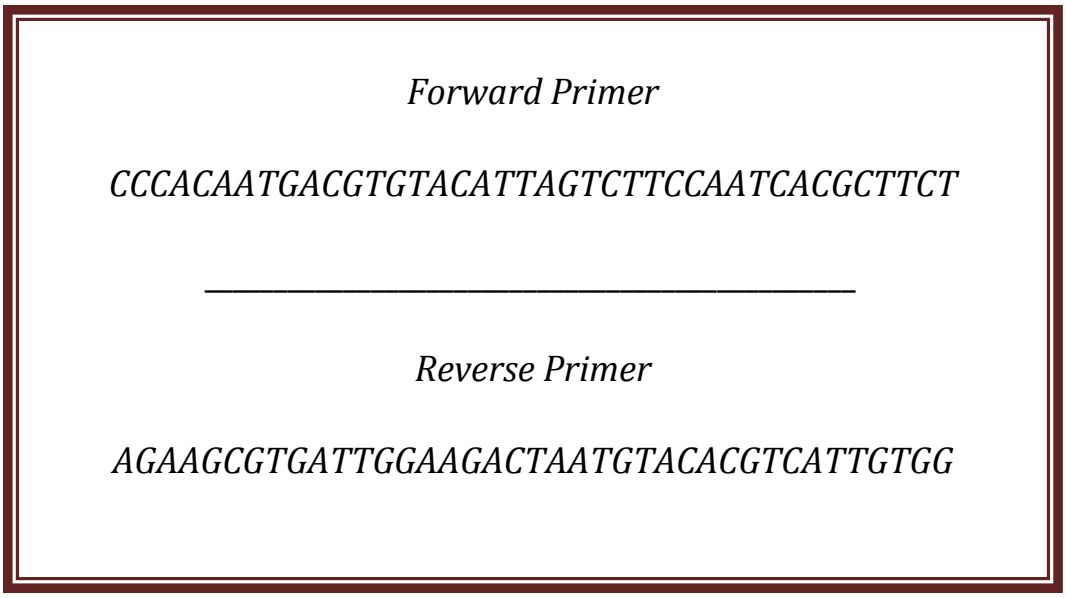

Figure 5, synthesized mutagenic primer sequences. These sequences match the sequence and reverse complement of the NES of PCV2b VP3.When the DNA strands of the GFP PCV2a VP3 construct are melted apart, these primers will anneal to the appropriate complement. When Pfu Turbo polymerase extends these primers, the resultant daughter DNA will be the chimeric mutant.

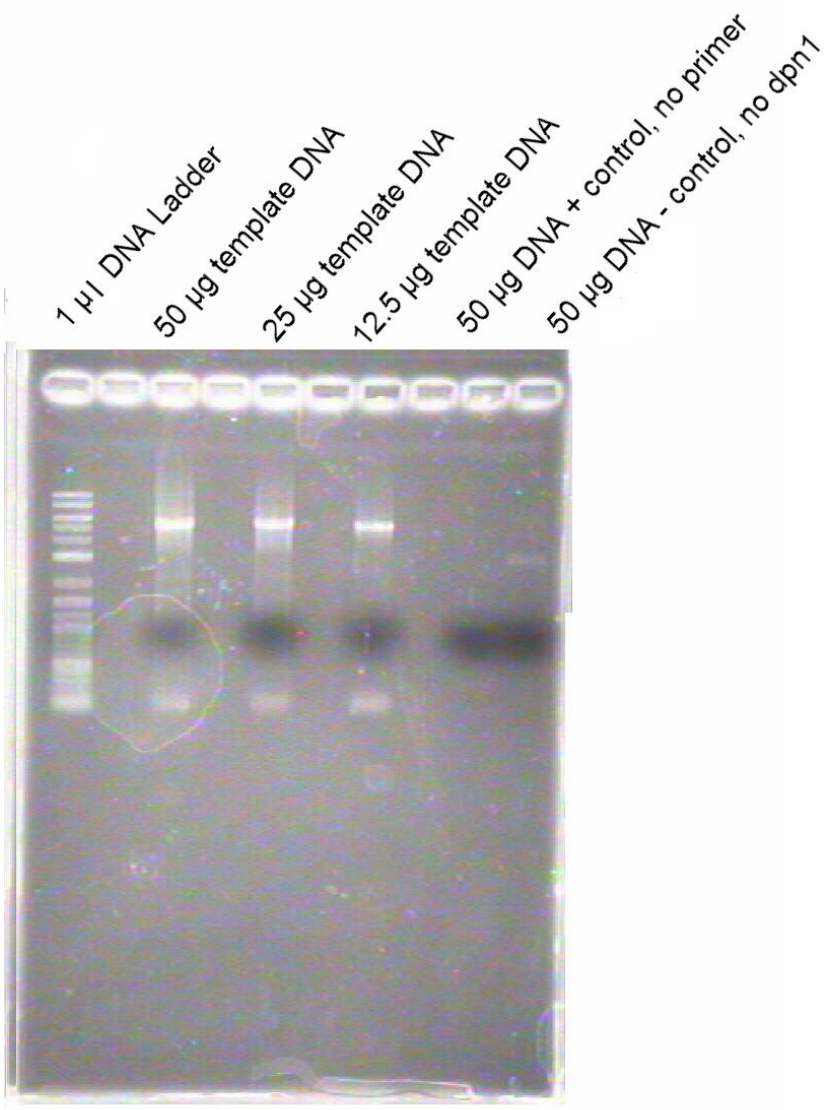

Figure 6, PCR Product gel. Top bands reside at around 4-5 kilobases, which is appropriately sized for the GFP PCV2VP3 construct, which is 5 kilobases in size. Bands at the bottom are likely digested template and leftover primer, corroborated by size around .1 kilobases.

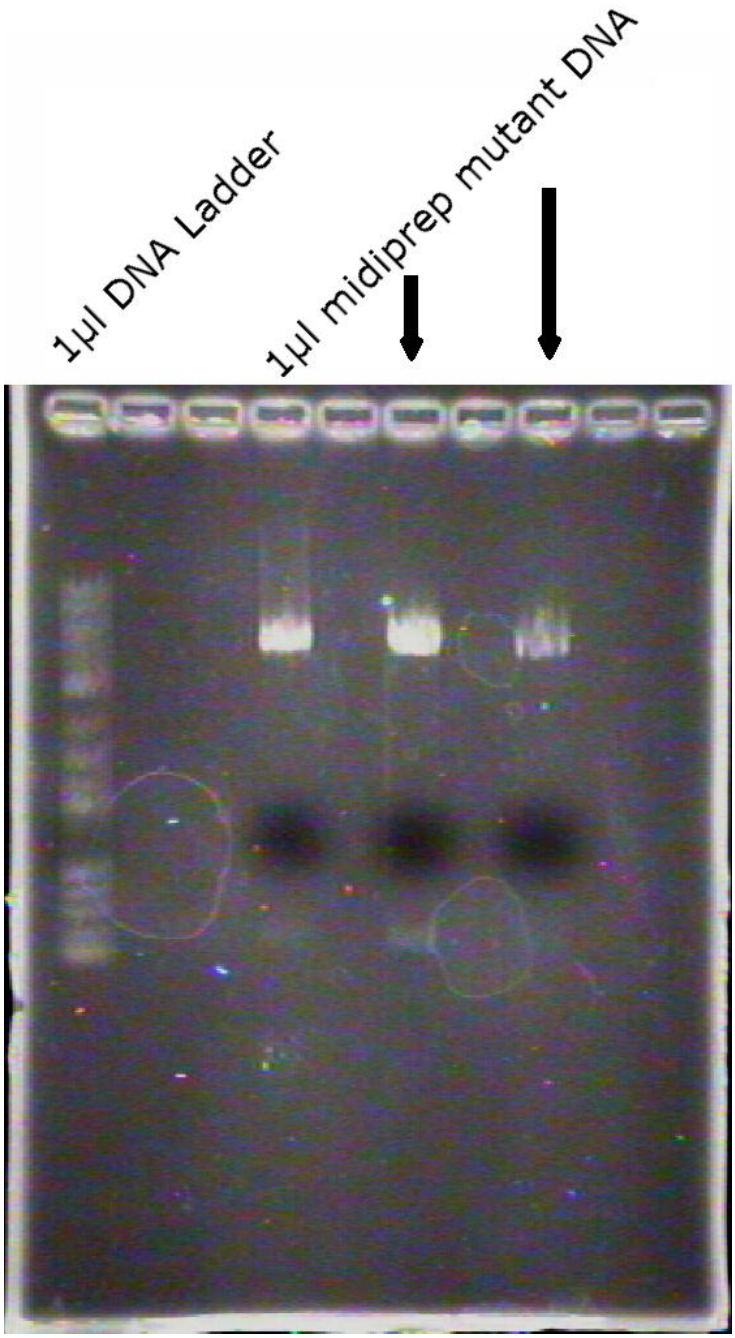

Figure 7, gel following midiprep and restriction. Top bands lie around 4-5 kilobases, while insert fragments are approximately 1-2 kilobases in length, confirming that PCR generated and amplified the mutant GFP PCV2 VP3 chimera. The size of the fragments predicted by restriction are 4.8 kilobases and 130 bases.

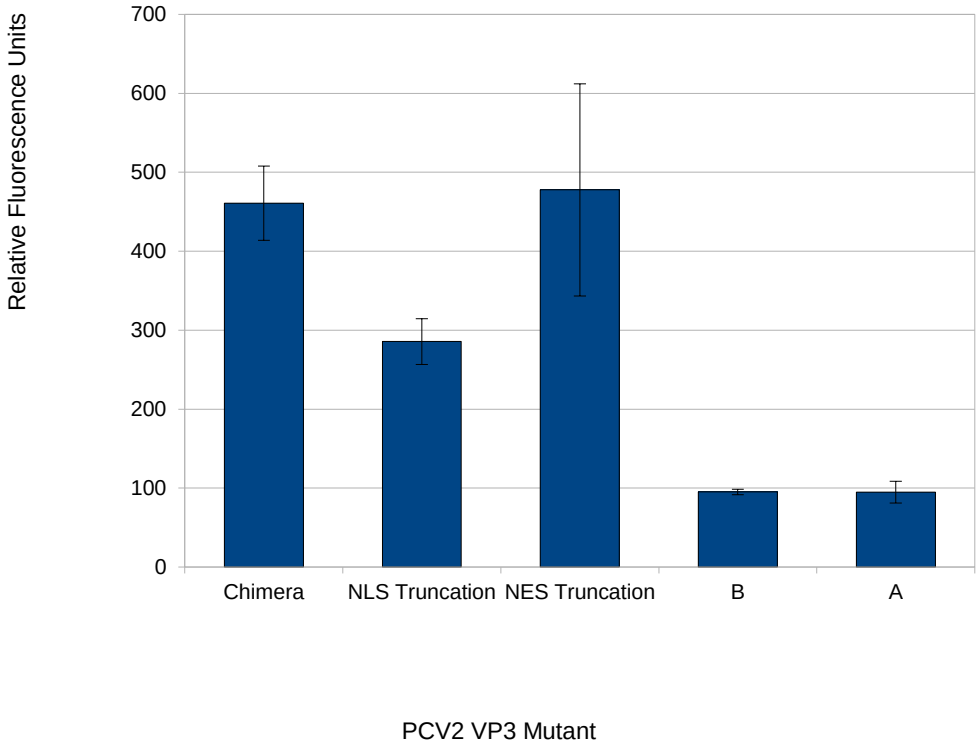

Figure 8, caspase apoptosis assay. The chimeric protein exhibited apoptotic capacity

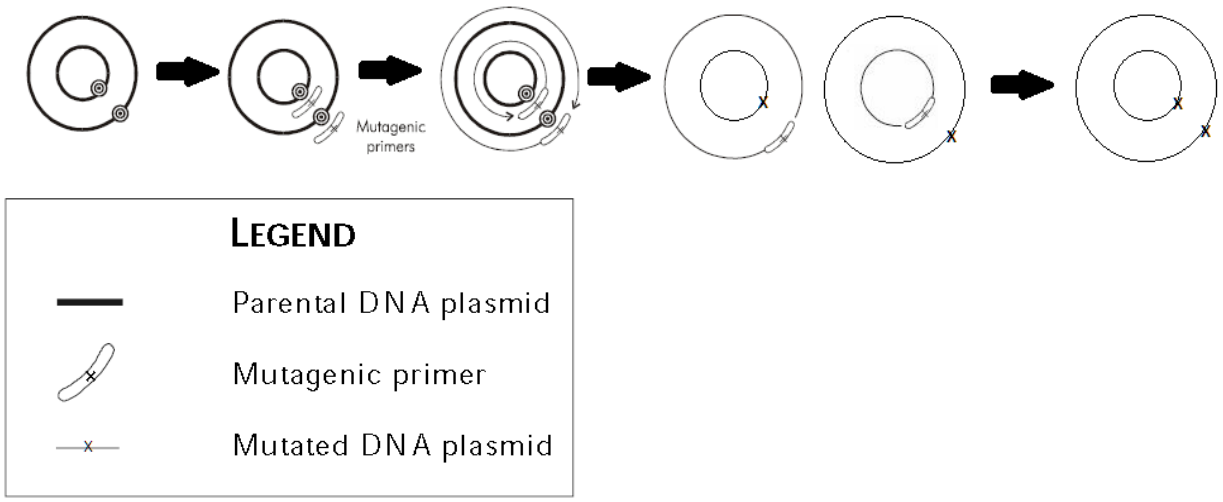

Figure 9, site-directed mutagenesis schematic.

References

1. Carter, G. *et al.* Circoviridae. *A Concise Review of Veterinary Virology* 1-4 (2006).

2. Chi-Ching, L. *et al.* Evidence for recombination in natural populations of porcine circovirus type 2 in Hong Kong and mainland China. *Journal of General Virology* 88, 1733-1737 (2007).

3. Nawagitgul, P. "Open Reading Frame 2 of Porcine Circovirus Type 2 Encodes a Major Capsid Protein." *Journal of General Virology* 81: 2281-287 (2000).

4. Dupont, K. *et al.* Genomic analysis of PCV2 isolates from Danish archives and a current PMWS case-control study supports a shift in genotypes with time. *Journal of Veterinary Microbiology* 128, 56-64 (2007).

5. Crowther, R. *et al.* Comparison of the Structures of Three Circoviruses: Chicken Anemia Virus, Porcine Circovirus Type 2, and Beak and Feather Disease Virus. *Journal of Virology* 77, 13036-13041 (2003).

6. Patterson, J. "A Study on the Severity and Relevance of Porcine Circovirus Type 2 Infections in Dutch Fattening Pigs with Respiratory Diseases." *Journal of Veterinary Microbiology* 142.3-4: 217-24 (2011).

7. Timmusk, S. "Porcine Circovirus Type 2 Replicase Binds the Capsid Protein and an Intermediate Filament-like Protein." *Journal of Virology* 87: 3215-223 (2006).

8. Liu, Jue. "The ORF3 Protein of Porcine Circovirus Type 2 Is Involved in Viral Pathogenesis in Vivo." *Journal of Virology* 80.10: 5065-073 (2006).

9. Cheung, A. *et al.* Exploring the genetic basis for porcine circovirus pathogenicity. *Journal of Virology* 152, 1035-1044 (2007).

10 Cheung, A. *et al.* Identification of an amino acid domain encoded by the capsid gene of porcine circovirus type 2 that modulates intracellular viral protein distribution during replication. *Virus Research* **155,** 358-362 (2011).

11. Cheung, A. *et al.* Identification of an amino acid domain encoded by the capsid gene of porcine circovirus type 2 that modulates intracellular viral protein distribution during replication. *Virus Research* **155,** 358-362 (2011).

12. Heilman, D. *et al.* Apoptin nucleocytoplasmic shuttling is required for cell type-specific localization, apoptosis, and recruitment of the anaphase-promoting complex/cyclosome to PML bodies. *Journal of Virology* 80, 7535-7545 (2006).

13. Russo, A. "Apoptosis: a Relevant Tool for Anticancer Therapy." *Annals of Oncology* 17.7: 115-23 (2006).

14. Leliveld, S. R., Y.-H. Zhang, L. R. Rohn, M. H. M. Noteborn, and J. P. Abrahams. Apoptin induces tumor-specific apoptosis as globular multimer. *J. Biol. Chem***.** 278**:** 9042-9051 **(**2003).

15. Liu, Jue. "Characterization of a Previously Unidentified Viral Protein in Porcine Circovirus Type 2-Infected Cells and Its Role in Virus-Induced Apoptosis." *Journal of Virology* 80.10: 8262-8274 (2004).

16. Liu, Jue. "The ORF3 Protein of Porcine Circovirus Type 2 Interacts with Porcine Ubiquitin E3 Ligase Pirh2 and Facilitates P53 Expression in Viral Infection." *Journal of Virology* 81.87: 9560-567 (2007).

17. Liu, Jue. "JNK and P38 Mitogen-Activated Protein Kinase Pathways Contribute to Porcine Circovirus Type 2 Infection." *Journal of Virology* 83.12: 6039-047 (2009).